Available online at www.sciencedirect.com
SCIENCE DIRECT®
Tetrahedron 60 (2004) 7141–7146
Tetrahedron

New β-linked pyrrole monomers: approaches to highly stable and conductive electrochromic polymers☆

Jocelyn M. Nadeau and Timothy M. Swager*

Department of Chemistry, Massachusetts Institute of Technology, 77 Massachusetts Avenue, Cambridge, MA 02139, USA

Received 8 May 2004; revised 25 May 2004; accepted 4 June 2004

Available online 2 July 2004

Abstract—An efficient synthetic route to β-linked dipyrrole monomers has been developed. Electrochemical polymerization of these monomers leads to the incorporation of polycyclic aromatic residues into a polymer backbone. The resulting conjugated polymer films are electroactive, robust electrochromic materials that are highly delocalized in their oxidized forms.

1. Introduction

The electron-rich nature of pyrrole typically imparts its polymer derivatives with desirable intrinsic redox properties such as low oxidation potential, high conductivity, and high redox stability. Although there are numerous studies on native polypyrrole,[1] and in contrast to the vast literature on functionalized polythiophenes,[2] there are relatively few examples of functionalized polypyrrole derivatives.[3] Herein we describe our recent progress toward incorporating pyrrole-based polycyclic aromatic units into a polymer backbone using the tandem cyclization/polymerization strategy depicted in Scheme 1 (X=NH; R=H). This work was inspired by previous studies in our group, which demonstrated that thiophene-based polycyclic aromatic residues could be incorporated into a conducting polymer backbone using this strategy (X=S; R=alkoxy groups).[4,5] Electrochemical studies of the resulting poly(naphthodithiophene)s revealed a new class of robust, electrochromic conducting polymers. In polymers of this architecture, the polycyclic aromatic core enforces planarity between adjacent heterocycles within the aromatic unit. Increased planarity leads to better π-overlap in the polymer thereby decreasing the bandgap and increasing conductivity. The β-linkage of the heterocycle to the benzene ring also increases π-overlap in the polymer backbone since fewer if any β-defects would be present due to steric constraints. The incorporation of pyrrole into such a scaffold is highly desirable as polypyrrole is inherently more conductive and better at stabilizing positive charge than simple polythiophene. Including polypyrrole's virtues in new conducting polymers offers potential performance enhancements that are needed in emerging organic electronic technologies. Such polymers could be used as antistatic coatings, in electrochromic devices, and, depending on the optical properties of the resulting polymers, as indium tin oxide replacement materials or optically transparent electrodes.

Herein we report a highly efficient synthetic route to β-linked dipyrrole monomers that can be used to generate families of conducting polymers with selected functionality. Electrochemical and spectroelectrochemical results reveal these materials to be highly electroactive and robust electrochromics.

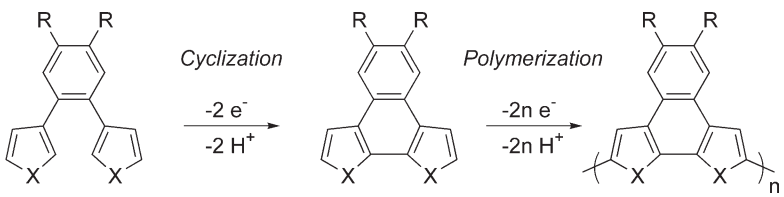

Scheme 1. Tandem cyclization/polymerization strategy toward conducting polymers.

☆ Supplementary data associated with this article can be found in the online version, at doi: 10.1016/j.tet.2004.06.016

Keywords: Conducting Polymers; Pyrrole; Electrochromic; Spectroelectrochemistry.
* Corresponding author. Tel.: +1-617-253-4423; fax: +1-617-253-7929; e-mail address: tswager@mit.edu

0040–4020/$ - see front matter © 2004 Elsevier Ltd. All rights reserved.
doi:10.1016/j.tet.2004.06.016

2. Results and discussion

2.1. Synthesis of β-dipyrrole monomers

Suzuki coupling methodology was used to generate new β-linked dipyrrole monomers **5** and **6** from readily available halogenated aromatics (Scheme 2). Palladium coupling methodology was selected for its versatility, as it allows for the generation of families of molecules for comparative studies. Other Pd coupling methods, i.e. Stille and Kumada, were explored, but yields were poor and irreproducible upon scale up. Electrophilic attack on pyrrole occurs preferentially at the α-position, so an indirect strategy developed by Muchowski and co-workers was used to install the boronic acid Pd coupling functionality at the β-position.[6,7] 1-(Triisopropylsilyl)pyrrole (1-TIPS-pyrrole) was brominated with NBS in THF to give 3-bromo-1-TIPS-pyrrole (**1**) in an 88% yield. Bromination at the β-position is favored because the steric bulk of the TIPS group blocks the more reactive α-sites. Boronic acid **2** was obtained by lithiation of **1** and quenching with $B(OCH_3)_3$ followed by an aqueous MeOH workup. Suzuki coupling of boronic acid **2** with 1,2-diiodobenzene and 3,4-dibromothiophene gave TIPS-protected β-dipyrrole monomers, **3** and **4**, respectively. The isolated yield of the coupling step was modest (40–80% yield) compared to typical yields observed for thiophene boronic acids.[4] Removal of the TIPS group with TBAF in THF generated the N–H functionality to give monomers **5** and **6** in 50–70% yield after purification. In addition to **5** and **6**, 1,3-di(pyrroyl)benzene (**8**)[8] was synthesized as a model compound to provide a monomer that is capable of electropolymerization but not intramolecular cyclization. Monomer **8** was obtained from 1,3-dibromobenzene in an overall 24% yield using the same methodology described above for **5** and **6** (Scheme 3).

2.2. Electrochemical polymerization of β-dipyrrole monomers 5 and 6

Electrochemical oxidation of monomer **5** was carried out to determine whether cyclization/polymerization occurs to give poly(**5**) (Scheme 4). Cyclic voltammetry (CV) of an electrolyte solution of dipyrrole monomer **5** and of poly(**5**) in a monomer-free electrolyte solution are shown in

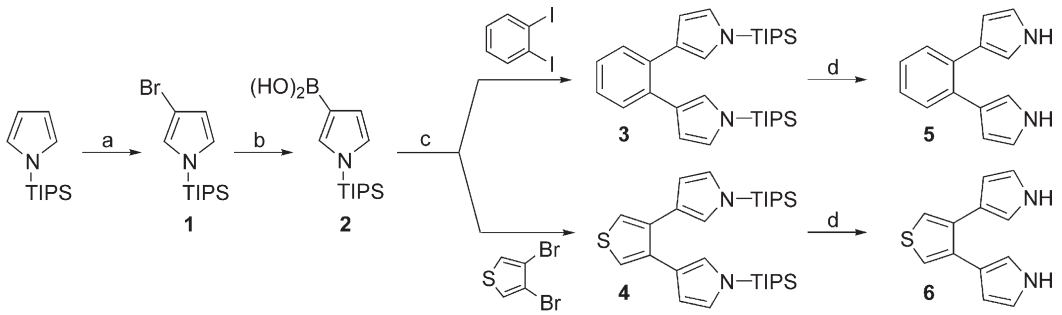

(a) NBS, THF, -78°C; 88%. (b) (i) *n*-BuLi, THF, -78°C. (ii) $B(OCH_3)_3$. (iii) 50% $MeOH_{(aq.)}$; ~50%.
(c) $Pd(PPh_3)_4$, 2M Na_2CO_3, MeOH, Tol., 80°C; 40-50%. (d) TBAF, THF; 50-75%.

Scheme 2. Synthetic route to β-linked dipyrrole monomers **5** and **6**.

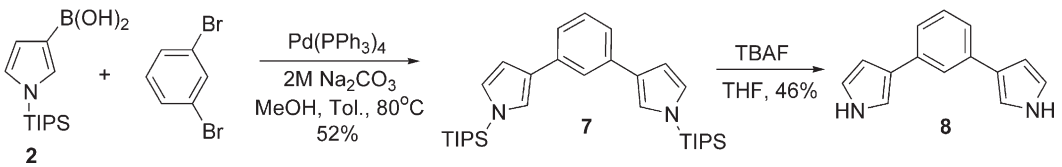

Scheme 3. Synthetic route to model monomer **8**.

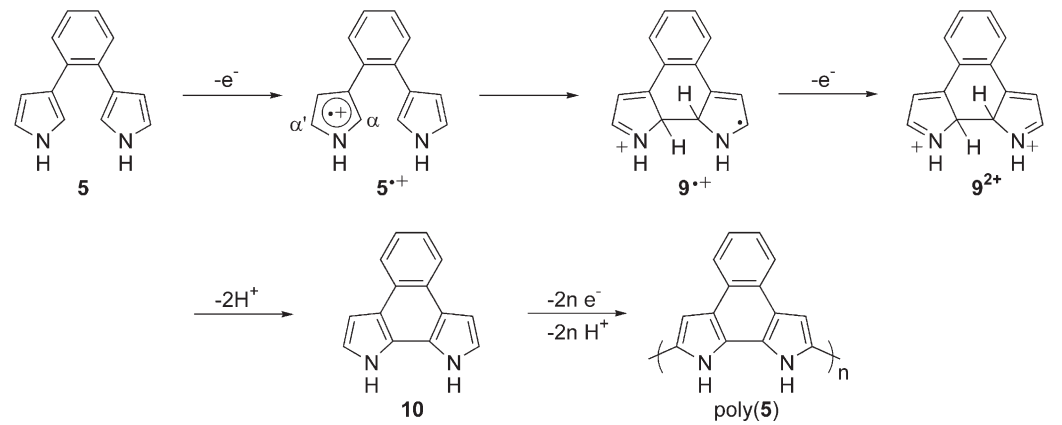

Scheme 4. Detailed mechanism proposed for oxidative cyclization/polymerization of monomer **5**.

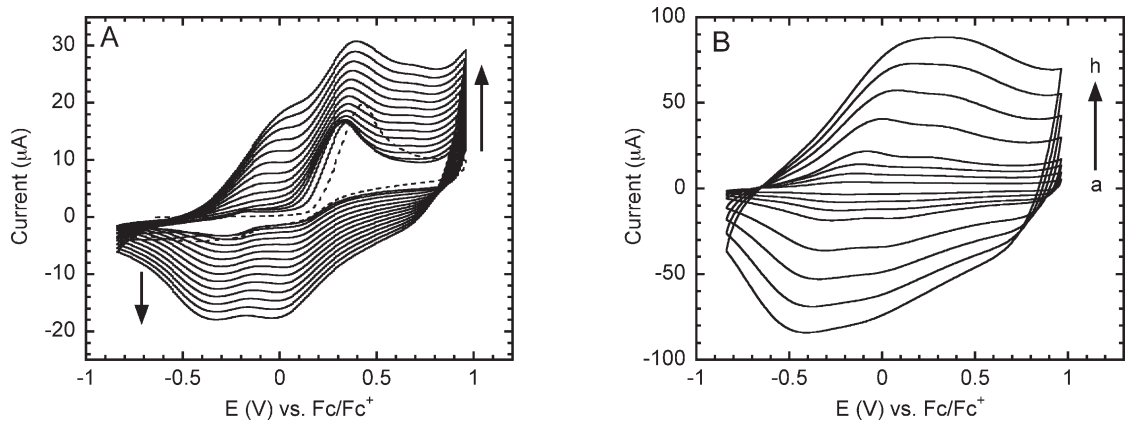

Figure 1. (A) Cyclic voltammetry of monomer **5** (~5 mM) in 0.1 M $TBAPF_6$ (CH_2Cl_2) cycled at 100 mV/s on a Pt button electrode; (B) cyclic voltammetry of resulting poly(**5**) in monomer-free electrolyte solution cycled at: (a) 25; (b) 50; (c) 75; (d) 100; (e) 200; (f) 300; (g) 400; (h) 500 mV/s.

Figure 1. Monomer **5** CV data (Fig. 1; Graph A) show only one distinct, irreversible oxidation wave during the first oxidative scan (dashed line; 0.45 V). Subsequent cycling leads to polymer deposition on the working electrode, as evidenced by the growth of lower-oxidation potential polymer-based redox activity that increases with successive scans. Scan rate dependence studies of poly(**5**) in a monomer-free electrolyte solution demonstrate that oxidation and reduction of the polymer is reversible (i.e., current scales linearly with scan rate) up to 500 mV/s (Fig. 1; Graph B). These results confirm that there is redox-active material confined to the electrode and that there are no significant kinetic barriers to charging and discharging of the film. In situ conductivity measurements for poly(**5**) grown on Pt interdigitated microelectrodes (IMEs) gave values of $0.38-1.2\times10^{-2}$ S cm^{-1}, suggesting that the polymer is highly conducting. Bulk conductivity values reported for polypyrrole are typically 10–100 S cm^{-1},[9] but in situ IME measurements typically give values that are 4–5 orders of magnitude smaller than bulk values due to the nature of the film coverage on the IME.[10] Conductivity values reported herein represent measurements made on IMEs that were not calibrated for uniform film thickness. Hence, the bulk conductivity of poly(**5**) is likely to actually be on the order of polypyrrole or better, but attempts to grow free-standing films of poly(**5**) to confirm this have yet to be successful.

We propose that oxidation of monomer **5** leads to intramolecular cyclization followed by polymerization to give poly(**5**) according to the mechanism outlined in Scheme 4. Removal of one electron from monomer **5** generates a radical cation on one pyrrole ring to give $\mathbf{5}^{\cdot+}$. The pyrrole radical cation reacts with the neighboring pyrrole ring to form a bond between the α-positions. Radical cation $\mathbf{9}^{\cdot+}$ would readily undergo a one-electron oxidation to give dication $\mathbf{9}^{2+}$. Subsequent loss of two protons from $\mathbf{9}^{2+}$ provides the cyclized product **10** that undergoes further oxidation to generate poly(**5**). It is also possible that $\mathbf{9}^{\cdot+}$ may shed one proton before undergoing additional oxidation; however such deprotonation reactions are generally slower than electron transfer. It could be argued that radical cation $\mathbf{5}^{\cdot+}$ might undergo reaction at the α′-position with another monomer in solution. However, the intramolecular reaction is likely to be favored entropically and formation of a polycyclic aromatic residue is likely to provide significant driving force. Moreover, there is some evidence that 3-phenylpyrroles react with electrophiles preferentially at the α-position versus the α′-position, although studies of this nature are limited.[11]

The CV data for monomer **5** show only one irreversible definable oxidation peak, although we initially expected two peaks representing the independent oxidations of **5** and **10**. However, given the very close potentials for the related oxidations in our earlier thiophene studies,[4,5] it seems likely that the two waves are simply unresolved. In order to address this issue directly, it would be desirable to synthesize cyclized monomer **10** to verify that its electropolymerization leads to a material with the same electrochemical behavior as poly(**5**). However, chemical oxidation of monomer **5** with $FeCl_3$ consistently led to the formation of intractable polymer, even at short reaction times. We further investigated whether treatment of TIPS-protected **3** with $FeCl_3$ produces the cyclized product since this monomer does not undergo electropolymerization. Only starting material **3** was isolated from the reaction mixture after a reductive anhydrous methanol quench and workup. We attribute this lack of reactivity to the steric bulk of the TIPS groups, which prevents the pyrrole rings from achieving coplanarity.

The cyclization/polymerization mechanism was also explored for monomer **6**. The redox behavior of monomer **6** and poly(**6**) is not as robust as that observed for monomer **5** and poly(**5**) (Fig. 2). The CV data for monomer **6** show a broad, irreversible overlapping oxidative peak in the first scan (dashed line in Fig. 2; Graph A) that is at a higher potential (0.67 V) than the analogous peak seen for monomer **5** (0.45 V). The higher potential is consistent with the larger angle (72°) between the pyrroles in **6**, which would impede its cyclization compared to **5** (60°). Further cycling leads to lower potential polymer-based redox activity. Unlike monomer **5**, successive scans typically leads to film passivation thwarting further polymer growth. Poly(**6**) CV data (Fig. 2; Graph B) show that its redox kinetics are reversible up to 300 mV/s. These results suggest that charge transport in poly(**6**) is not as efficient as in poly(**5**). In situ conductivity measurements on uncalibrated IMEs for poly(**6**) gave values of $0.18-1.5\times10^{-3}$ S cm^{-1}.

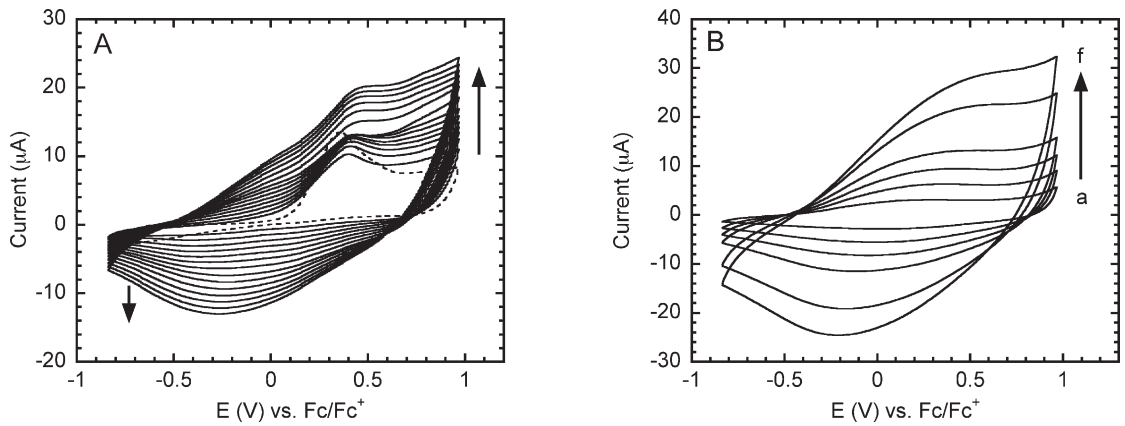

Figure 2. (A) Cyclic voltammetry of monomer **6** (~5 mM) in 0.1 M $TBAPF_6$ (CH_2Cl_2) cycled at 100 mV/s on a Pt button electrode; (B) cyclic voltammetry of resulting poly(**6**) in monomer-free electrolye solution cycled at: (a) 25; (b) 50; (c) 75; (d) 100; (e) 200; (f) 300 mV/s.

Collectively, these results suggest that poly(**6**) is not as conductive as poly(**5**). It might be that this monomer does not fully cyclize and may also undergo competitive polymerization through the redox-active thiophene, thereby leading to defects in the polymer backbone.

2.3. Spectroelectrochemistry and coulometry

Spectroelectrochemistry is a useful technique for studying conducting polymers, as it allows one to study changes in absorption spectra as a function of applied voltage. This technique was used to evaluate the electrochromicity, charge delocalization and related donor–acceptor transitions that will arise from proximate neutral and oxidized segments in poly(**5**), poly(**6**), and poly(**8**) (Fig. 3; Graphs A, B, and C, respectively). Oxidation of conducting polymers leads to charge delocalization along the polymer backbone, which gives rise to changes in the polymer's optical transitions. As shown for poly(**5**) in Figure 4, the neutral polymer is composed of isolated aromatic pyrrole units. Oxidation of the polymer leads to a structure with increased quinoidal character, which facilitates charge delocalization along the polymer backbone. This charge delocalization results in a red shift of the polymer's absorption spectrum. The extent of the red shift upon oxidation is a measure of the degree of charge delocalization.

Neutral poly(**5**) is yellow and shows a broad absorption centered at 3.2 eV (Fig. 3; Graph A). Oxidation to its conducting form results in a red shift where an intermediate band at 2.3 eV gives way to a broad band that extends from the visible out into the near-IR region (NIR region <1.6 eV). Not surprisingly, oxidized poly(**5**) is black, owing to its significant absorption in the visible region.

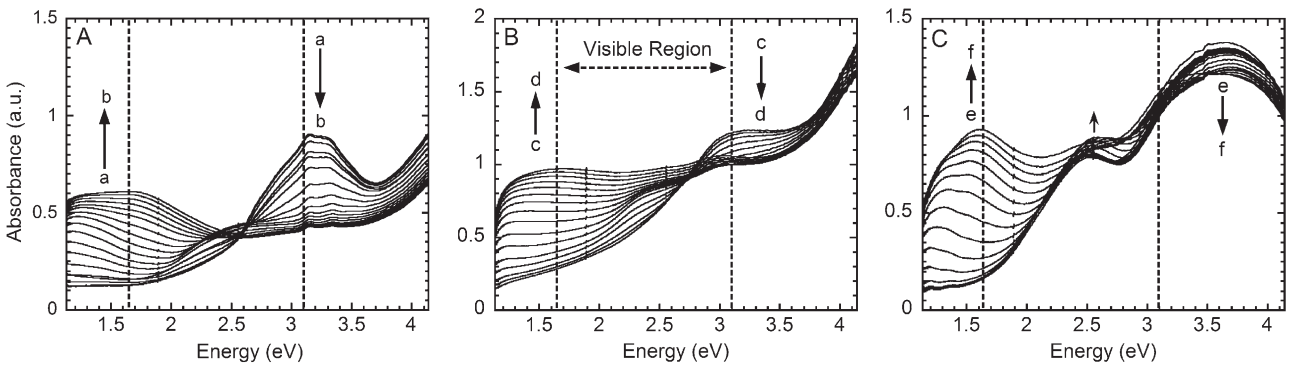

Figure 3. Spectroelectrochemical data for thin polymer films grown on ITO-coated glass. The experiment was conducted in 0.1 M $TBAPF_6$ (CH_2Cl_2) using 100 mV steps within the following potential windows: (A) poly(**5**) (a and b) −0.93 to +0.78 V; (B) poly(**6**) (c and d) −0.83 to +0.98 V; and (C) poly(**8**) (e and f) −0.93 to +0.98 V.

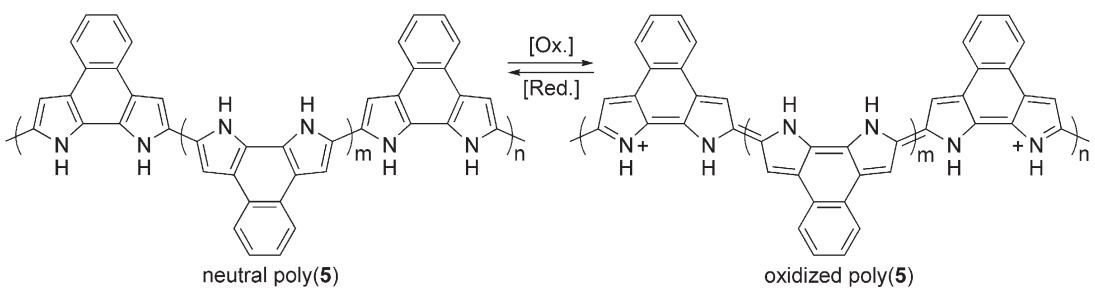

Figure 4. Structures of neutral and oxidized forms of poly(**5**).

Neutral poly(**6**) is yellowish-mauve with a broad absorption at 3.1 eV (Fig. 3; Graph B). Oxidation of poly(**6**) also gives a black film, and the absorption band shifts to a weak intermediate band at 2.3 eV that disappears upon further oxidation to give a broad, lower energy band that spans the visible and extends into the NIR region. The spectroelectrochemical data for poly(**5**) and poly(**6**) are actually quite similar, implying that they have similar structures; however, poly(**5**) is more delocalized as its low-energy band extends further into the NIR region. Poly(**5**) and poly(**6**) both appear to favor a highly delocalized structure in their oxidized forms. Monomer **8** was used as a model because it can electropolymerize, but the pyrrole units are too far apart to undergo intramolecular cyclization (see Supporting information for CV data on monomer **8** and poly(**8**)). Neutral poly(**8**) has two bands centered at 3.7 and 2.6 eVs. Upon oxidation, the former band decreases slightly and the latter increases slightly, which is attended by the appearance of a relatively sharp visible/NIR absorption band that is higher energy than the analogous peak observed for poly(**5**) and poly(**6**). Collectively, these results suggest that the degree of charge delocalization in the polymer backbone decreases in the following order: poly(**5**)>poly(**6**)>poly(**8**). It is likely that poly(**6**) is only partially cyclized within the polymer, which leads to interruption in π-overlap and decreased delocalization.

We were interested to see if our polycyclic pyrrole polymers are capable of displaying improved charge storage capacity relative to polypyrrole. To assess this, we used the amount of irreversible charge integrated through the polymerization to determine the number of moles of monomers deposited on the electrode. Oxidation of polypyrrole leads to one cationic charge for every 3–4 repeating units.[12] We have compared the charge storage capacity of poly(**5**), poly(**6**), and poly(**8**) to that of polypyrrole when oxidized at +0.98 V and find that poly(**5**) and poly(**8**) have equivalent charge storage capacity to polypyrrole determined under identical conditions. Poly(**6**) exhibited a 30% higher charge storage capacity per pyrrole despite its less conductive nature. This improved charge storage capacity reflects the electron rich nature of the thiophene moiety in poly(**6**) relative to the benzene subunit in poly(**5**) and poly(**8**).

3. Conclusions

We have developed an efficient synthetic route to β-linked dipyrrole monomers using Suzuki coupling methodology. Electrochemical oxidation of these monomers leads to the incorporation of polycyclic aromatic residues into a polymer backbone to give highly robust, electrochromic conducting polymers.

4. Experimental

4.1. General comments

^{1}H and ^{13}C NMR spectra were determined at 300 MHz using a Varian Mercury-300 spectrometer and are referenced to residual $CHCl_3$ (7.27 ppm for ^{1}H and 77.23 ppm for ^{13}C). Melting points are uncorrected. High-resolution mass spectra (HRMS) were determined at the MIT Department of Chemistry Instrumentation Facility (DCIF) on a Bruker Daltronics APEX II 3 Tesla FT-ICR-MS. Elemental analysis was conducted at Quantitative Technologies, Inc. (Whitehouse, NJ). Compounds **1** and **2** were synthesized according to literature methods.[6,7] All air and water sensitive synthetic manipulations were performed under an argon atmosphere using standard Schlenk techniques. Tetrahydrofuran (THF), toluene, and dichloromethane (CH_2Cl_2) were passed through activated alumina prior to storage under an inert atmosphere (Innovative Technologies, Inc.). All electrochemical measurements were made with an Autolab II with PGSTAT 30 potentiostat (Eco Chemie). Cyclic voltammetry was performed at a Pt button electrode in an argon-purged, one chamber/three electrode cell. The reference electrode was a quasi-internal Ag wire (BioAnalytical Systems) submersed in 0.01 M $AgNO_3$/0.1 M $TBAPF_6$ in anhydrous acetonitrile, and a Pt coil or flag was used as the counter electrode. All potentials are referenced to the Fc/Fc^+ redox couple. All experiments were conducted in 0.1 M $TBAPF_6$ in CH_2Cl_2 under ambient laboratory conditions. In situ conductivity measurements were performed on polymer films grown on 5 μm Pt interdigitated microelectrodes (Abtech Scientific, Inc.) and are uncalibrated. Spectroelectrochemistry was carried out on polymer films deposited on indium-tin oxide (ITO) coated glass, and absorption spectra were determined on an Agilent 8453 diode array spectrophotometer.

4.1.1. 1,2-Di(1-triisopropylsilyl-3-pyrroyl)benzene (3). A 50 mL Schlenk flask was charged with 1-TIPS-pyrrole-3-boronic acid (**2**) (5.0 g; 19 mmol), 1,2-diiodobenzene (627 mg; 1.9 mmol), toluene (10 mL), methanol (10 mL), and 2.0 M Na_2CO_3 (1 mL). The solution was purged with argon for 5 min followed by addition of $Pd(PPh_3)_4$ (44 mg; 0.038 mmol) under a positive flow of argon. The flask was sealed, and the reaction was heated at 80 °C for 4 h. Upon cooling to room temperature, the reaction mixture was washed with water, and the aqueous layer was extracted with ethyl acetate. The organic layers were combined, dried over $MgSO_4$, filtered, and concentrated under reduced pressure. The crude product was purified by column chromatography on silica gel (20% CH_2Cl_2 in hexanes) followed by recrystallization from $EtOH/H_2O$ to give a colorless, crystalline solid (420 mg; 42% yield): mp 89–91 °C; ^{1}H NMR (300 MHz; $CDCl_3$) δ 1.09 (d, J=7.5 Hz, 36H), 1.40 (sept, J=7.5 Hz, 6H), 6.26–6.28 (m, 2H), 6.65–6.67 (m, 2H), 6.68–6.69 (m, 2H), 7.20 (dd, J=3.3, 5.7 Hz, 2H), 7.42 (dd, J=3.3, 5.7 Hz, 2H); ^{13}C NMR (300 MHz; $CDCl_3$) δ 11.86, 18.07, 111.71, 123.21, 123.50, 125.94, 127.11, 130.21, 134.95. MS (ESI) exact mass calculated for $C_{32}H_{52}N_2Si_2$ $[M+Na]^+$ 543.3561, found 543.3576. Repeated attempts to obtain elemental data were unsuccessful as the carbon number was consistently low; however, the hydrogen and nitrogen data were always within the accepted limits (calculated H, 10.06; N, 5.38, found H, 10.15; N, 5.37).

4.1.2. 3,4-Di(1-triisopropylsilyl-3-pyrroyl)thiophene (4). Prepared as described for **3** from 3,4-dibromothiophene (298 mg; 1.23 mmol) to give a colorless crystalline solid (39% yield): mp 99–101 °C; ^{1}H NMR (300 MHz; $CDCl_3$) δ

1.09 (d, J=7.2 Hz, 36H), 1.40 (sept, J=7.5 Hz, 6H), 6.37–6.38 (m, 2H), 6.70–6.73 (m, 4H), 7.16 (s, 2H); ^{13}C NMR (300 MHz; $CDCl_3$) δ 11.80, 18.02, 111.29, 120.83, 122.15, 122.75, 123.85, 136.65. MS (EI) exact mass calculated for $C_{30}H_{50}N_2SSi_2$ $[M]^+$ 526.3228, found 526.3205. Anal. calculated for $C_{30}H_{50}N_2SSi_2$: C, 68.38; H, 9.56; N, 5.32; S, 6.08. Found, C, 68.37; H, 9.81; N, 5.21; S, 6.22.

4.1.3. 1,3-Di(1-triisopropylsilyl-3-pyrroyl)benzene (7). Prepared as described for **3** from 1,3-dibromobenzene to give a colorless crystalline solid (52% yield): mp 155–156 °C; ^{1}H NMR (300 MHz; $CDCl_3$) δ 1.16 (d, J=7.2 Hz, 36H), 1.51 (sept, J=7.5 Hz; 6H), 6.67–6.69 (m, 2H), 6.83–6.85 (m, 2H), 7.10–7.11 (m, 2H), 7.28–7.39 (m, 3H), 7.72–7.73 (m, 1H); ^{13}C NMR (300 MHz; $CDCl_3$) δ 11.90, 18.07, 109.04, 120.89, 122.67, 122.79, 125.26, 127.40, 128.88, 136.46. MS (ESI) exact mass calculated for $C_{32}H_{52}N_2Si_2$ $[M+H]^+$ 521.3742, found 521.3724.

4.1.4. 1,2-Di(3-pyrroyl)benzene (5). A 1.0 M solution of TBAF in THF (1.7 mL; 1.7 mmol) was added to **3** (420 mg; 0.82 mmol) dissolved in THF. The reaction was stirred at room temperature under argon for 15 min. The solvent was removed under reduced pressure, and the crude product was purified by column chromatography on silica gel (20% hexanes in CH_2Cl_2) to give a colorless oil that crystallized upon standing (132 mg; 78% yield): mp 95–96 °C; ^{1}H NMR (300 MHz; $CDCl_3$) δ 6.20–6.22 (m, 2H), 6.65–6.67 (m, 2H), 6.72–6.74 (m, 2H), 7.25 (dd, J=3.3, 5.4 Hz, 2H), 7.44 (dd, J=3.3, 5.4 Hz, 2H), 8.08 (br s, 2H); ^{13}C NMR (300 MHz; $CDCl_3$) δ 109.74, 116.86, 117.30, 124.99, 126.24, 130.24, 135.02. MS (ESI) exact mass calculated for $C_{14}H_{12}N_2$ $[M+Na]^+$ 231.0893, found 231.0897.

4.1.5. 3,4-Di(3-pyrroyl)thiophene (6). Prepared as described for **5** from compound **4** to give a colorless oil (50% yield): ^{1}H NMR (300 MHz; $CDCl_3$) δ 6.28–6.31 (m, 2H), 6.73–6.77 (m, 4H), 7.18 (s, 2H), 8.18 (br s, 2H); ^{13}C NMR (300 MHz; $CDCl_3$) δ 109.34, 116.47, 117.58, 120.11, 121.26, 136.46. MS (ESI) exact mass calculated for $C_{12}H_{10}N_2S$ $[M]^+$ 215.0637, found 215.0646.

4.1.6. 1,3-Di(3-pyrroyl)benzene (8). Prepared as described for **5** from compound **7** to give a colorless oil (46% yield): ^{1}H NMR (300 MHz; $CDCl_3$) δ 6.60–6.62 (m, 2H), 6.85–6.88 (m, 2H), 7.13–7.15 (m, 2H), 7.31–7.40 (m, 3H), 7.72–7.73 (m, 1H), 8.28 (br s, 2H); ^{13}C NMR (300 MHz; $CDCl_3$) δ 106.91, 114.82, 118.99, 122.64, 122.98, 125.45, 129.07, 136.22. MS (ESI) exact mass calculated for $C_{14}H_{12}N_2$ $[M]^+$ 209.1073, found 209.1076.

Acknowledgements

The authors are grateful for financial support provided by the Army Research Office's Tunable Optical Polymers MURI program and for the use of resources provided by the Institute for Soldier Nanotechnologies, also funded by the Army Research Office.

References and notes

1. (a) In *Handbook of Conducting Polymers*; 2nd ed. Skotheim, T. A., Elsenbaumer, R. L., Reynolds, J. R., Eds.; Marcel Dekker: New York, 1998. (b) Sadki, S.; Schottland, P.; Brodie, N.; Sabouraud, G. *Chem. Soc. Rev.* **2000**, *29*, 283–293.
2. (a) Roncali, J. *Chem. Rev.* **1992**, *92*, 711–738. (b) McCullough, R. D. *Adv. Mater.* **1998**, *10*, 93–116.
3. (a) Deronzier, A.; Moutet, J. C. *Acc. Chem. Res.* **1989**, *22*, 249–255. (b) Masuda, H.; Kaeriyama, K. *Synth. Met.* **1990**, *38*, 371–379. (c) Chen, J.; Too, C. O.; Wallace, G. G.; Swiegers, G. F.; Skelton, B. W.; White, A. H. *Electrochim. Acta* **2002**, *47*, 4227–4238. (d) Lee, D.; Swager, T. M. *J. Am. Chem. Soc.* **2003**, *125*, 6870–6871. (e) Groenendaal, L.; Zotti, G.; Aubert, P. H.; Waybright, S. M.; Reynolds, J. R. *Adv. Mater.* **2003**, *15*, 855–879. (f) Godillot, P.; Youssoufi, H. K.; Srivastava, P.; El Kassmi, A.; Garnier, F. *Synth. Met.* **1996**, *83*, 117–123.
4. Tovar, J. D.; Swager, T. M. *Adv. Mater.* **2001**, *13*, 1775–1780.
5. Tovar, J. D.; Rose, A.; Swager, T. M. *J. Am. Chem. Soc.* **2002**, *124*, 7762–7769.
6. Bray, B. L.; Mathies, P. H.; Naef, R.; Solas, D. R.; Tidwell, T. T.; Artis, D. R.; Muchowski, J. M. *J. Org. Chem.* **1990**, *55*, 6317–6328.
7. Alvarez, A.; Guzman, A.; Ruiz, A.; Velarde, E.; Muchowski, J. M. *J. Org. Chem.* **1992**, *57*, 1653–1656.
8. Fumoto, Y.; Uno, H.; Tanaka, K.; Tanaka, M.; Murashima, T.; Ono, N. *Synthesis* **2001**, *3*, 399–402.
9. Diaz, A. F.; Castillo, J. I.; Logan, J. A.; Lee, W. Y. *J. Electroanal. Chem.* **1981**, *129*, 115–132.
10. Kingsborough, R. P.; Swager, T. M. *Adv. Mater.* **1998**, *10*, 1100–1104.
11. Balasubramanian, T.; Strachan, J. P.; Boyle, P. D.; Lindsey, J. S. *J. Org. Chem.* **2000**, *65*, 7919–7929.
12. (a) Kanazawa, K. K.; Diaz, A. F.; Geiss, R. H.; Gill, W. D.; Kwak, J. F.; Logan, J. A.; Rabolt, J. F.; Street, G. B. *J. Chem. Soc. Chem. Commun.* **1979**, 854–855. (b) Diaz, A. F.; Castillo, J. I. *J. Chem. Soc. Chem. Commun.* **1980**, 397–398.